

Refractive index of erbium doped GaN thin films

S. Alajlouni,¹ Z. Y. Sun,¹ J. Li,¹ J. M. Zavada,² J. Y. Lin,¹ and H. X. Jiang^{1,a)}

¹Department of Electrical and Computer Engineering, Texas Tech University, Lubbock, Texas 79409, USA

²Department of Electrical and Computer Engineering, Polytechnic Institute of New York University, Brooklyn, New York 11201, USA

(Received 19 June 2014; accepted 14 August 2014; published online 25 August 2014)

GaN is an excellent host for erbium (Er) to provide optical emission in the technologically important as well as eye-safe 1540 nm wavelength window. Er doped GaN (GaN:Er) epilayers were synthesized on c-plane sapphire substrates using metal organic chemical vapor deposition. By employing a pulsed growth scheme, the crystalline quality of GaN:Er epilayers was significantly improved over those obtained by conventional growth method of continuous flow of reaction precursors. X-ray diffraction rocking curve linewidths of less than 300 arc sec were achieved for the GaN (0002) diffraction peak, which is comparable to the typical results of undoped high quality GaN epilayers and represents a major improvement over previously reported results for GaN:Er. Spectroscopic ellipsometry was used to determine the refractive index of the GaN:Er epilayers in the 1540 nm wavelength window and a linear dependence on Er concentration was found. The observed refractive index increase with Er incorporation and the improved crystalline quality of the GaN:Er epilayers indicate that low loss GaN:Er optical waveguiding structures are feasible. © 2014 AIP Publishing LLC. [<http://dx.doi.org/10.1063/1.4893992>]

The intra-4f transitions of Er³⁺ ions lead to emissions at 1.54 μm which overlap with the minimum optical loss region of silica fibers used in optical communications. Consequently, extensive research has been devoted to the studies of Er incorporation into various hosts including optical fibers and semiconductor materials.^{1–7} One of the goals has been to combine the high functionality and compactness of semiconductor devices with the high information carrying capability of optical fiber networks.^{5–17} The desired optical emission line at 1.54 μm from Er doped semiconductors with narrow bandgaps, such as silicon, has a low efficiency at room temperature due to a strong thermal quenching effect. In general, the thermal stability of Er emissions at 1.54 μm increases as the energy bandgap of the semiconductor host increases.⁸ Over the last 20 yr, a number of research groups have studied materials growth and basic properties of Er doped III-nitride semiconductors, which are expected to be excellent host materials for Er ions due to their structural properties and wide bandgaps.^{9–17}

In addition to the wide interest stemming from photonic integrated circuits and optical communications, Er doped GaN semiconductor crystals (GaN:Er) have the potential to be an excellent gain medium for high energy lasers (HELs) operating in the eye-safer 1.54 μm spectral region. GaN has outstanding optical, mechanical, and thermal conductivity properties to withstand the severe operating conditions of HEL. In addition, a high Er doping level, above 10²¹ cm⁻³, is attainable in GaN,¹⁴ which is three to four orders of magnitude higher than the typical doping level in Er-doped glass.

It is important to characterize the change of index of refraction of GaN:Er due to Er incorporation for many photonic device applications. Our studies have focused on GaN:Er epilayers grown by metal organic chemical vapor

deposition (MOCVD). In an optical waveguide, the optical gain (G) is expressed as¹⁸

$$G = \Gamma(g - \alpha)L, \quad (1)$$

where Γ , g , α , and L refer to the confinement factor, gain coefficient, optical attenuation, and length of the waveguide, respectively. In our previous work, the optical loss in GaN:Er waveguides was shown to be correlated with the linewidth of the GaN (0002) x-ray diffraction (XRD) rocking curves in ω -scan. More specifically, the optical attenuation coefficient α increased almost linearly with an increase of the full width at half maximum (FWHM) of the GaN (0002) XRD rocking curve.¹⁹ This increase in the FWHM is an indication of the presence of a larger number of threading dislocations in GaN:Er epilayers that act as light scattering centers. Experimental results indicated that a FWHM < 380 arc sec is required in order to achieve GaN:Er waveguides with an optical loss less than 1 dB/cm. Previously, the attainable FWHM of GaN (0002) XRD rocking curves of GaN:Er epilayers deposited on sapphire substrate has been greater than 400 arc sec,^{19–21} which is significantly larger than those of the typical undoped high quality GaN epilayers grown on sapphire substrate (~300 arc sec).²² Consequently, finding effective methods to reduce the dislocation density in GaN:Er is necessary in order to realize low loss optical devices. In addition, the confinement factor Γ depends on the difference between refraction index of the active material and the surrounding media.

In this work, we report the use of a pulsed precursor flow MOCVD growth method for obtaining GaN:Er epilayers with significantly improved crystalline quality as determined by XRD measurements. The improved material quality also allowed characterization of the refractive index of GaN:Er epilayers in the 1.54 μm wavelength window with a high accuracy. Our results indicate that the refractive index

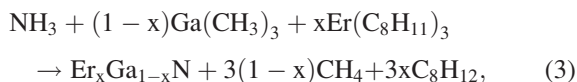
^{a)}hx.jiang@ttu.edu

of GaN:Er increases almost linearly with the Er doping concentration (N_{Er}). This finding implies a higher confinement factor can be achieved for waveguides with highly doped GaN:Er layers. Furthermore, the realization of improved crystalline quality via the pulsed growth method is expected to provide a dramatic reduction in the optical loss in GaN:Er based waveguides. The combination of enhanced confinement factor and reduced optical loss reinforces the potential of GaN:Er for $1.54\ \mu\text{m}$ waveguide amplifier and laser applications.

GaN:Er epilayers of $0.6\ \mu\text{m}$ in thickness were grown on *c*-plane sapphire substrates using pulsed flow MOCVD. The growth of these epilayers began with a thin GaN buffer layer, followed by a $1.5\ \mu\text{m}$ undoped GaN epilayer template grown at 1040°C and a $0.6\ \mu\text{m}$ GaN:Er epilayer. Thickness of epilayers was monitored using *in-situ* interferometer. Trimethylgallium (TMGa) and ammonia (NH_3) were used as group-III and group-V precursors, respectively. Triisopropyl cyclopentadienyl-erbium (TRIPeR) was used as the *in-situ* Er doping precursor. Precursors were carried by hydrogen gas (H_2) into the MOCVD reactor which was set at 1000°C and a pressure of 20 Torr. The typical attainable FWHM of the GaN (0002) XRD rocking curve of GaN:Er epilayers has been larger than 400 arc sec, which rendered an optical loss $>6\ \text{dB/cm}$ in GaN:Er based optical waveguides.¹⁹ We speculate that the pre-reaction between TRIPeR and NH_3 in the gas phase could be a cause of the degraded crystalline quality upon Er doping, similar to the pre-reaction between NH_3 and trimethylaluminum during AlN epilayer growth.^{23–25} When NH_3 and TRIPeR are mixed in the injection area of the MOCVD reactor, they will react to form an adduct according to the following chemical reaction:



The adduct has a low vapor pressure, which makes the transport of Er into the reaction zone difficult. To overcome this problem to certain degree, we supplied NH_3 and the TRIPeR through separated lines to avoid the pre-mixing of NH_3 and TRIPeR precursors before injection into the reactor. In addition, we adopted a pulsed precursor flow growth scheme developed for AlN epilayer growth^{23–25} to further reduce the chance of pre-reaction by flowing NH_3 in one pulse and then flowing TMGa and TRIPeR in another pulse. A phase shift epitaxy scheme was also used for the growth of Eu doped GaN by MBE to separate the optimization process of host lattice growth from doping.²⁶ In the high temperature growth area of the MOCVD reactor, the chemical reaction of GaN:Er epilayer growth can be described by the following equation:



where x denotes the Er doping concentration in GaN. In the pulsed growth process, at a given growth temperature, there are at least 6 basic parameters that need to be optimized, “on” time for NH_3 flow, “on” time for TMGa flow, “on” time for TRIPeR flow, and their respective flow rates.

Figure 1 shows the optimum flow rates and pulse sequence employed to obtain the GaN:Er epilayer with the lowest FWHM of the (0002) XRD rocking curve. Due to the low vapor pressure of the Er (TRIPeR) precursor, it takes a few seconds to stabilize the flow of the TRIPeR mass flow controller. As such, a tradeoff must be considered while employing the pulsed growth method. In the optimized growth scheme shown in Fig. 1, 3 s of overlap between NH_3 pulse and TRIPeR pulse were employed to stabilize the flow of the TRIPeR mass flow controller before flowing TMGa.

To study the impact of the pulsed MOCVD method, three GaN samples were grown: one un-doped sample and two GaN:Er samples. The pulsed growth sequences for the two GaN:Er samples (pulsed growth-1 and pulsed growth-2) were identical except that the TRIPeR flow rates were different. The Er concentrations of these samples, $\sim 1.3 \times 10^{20}$ and 3.6×10^{20} , were calibrated using secondary ion mass spectrometry (SIMS) conducted by Evans Analytical Group. For comparison, GaN:Er epilayers were also grown under continuous flow of reaction precursors. In Fig. 2 the XRD rocking curves of the GaN (0002) diffraction peak for GaN:Er epilayers grown with pulsed and continuous flow methods are compared. The pulsed growth method leads to FWHMs of less than 300 arc sec for GaN:Er epilayers. This is a major improvement over the conventional continuous flow growth method which produced a FWHM of 450 arc sec. Figure 3 shows the room temperature photoluminescence (PL) spectra of two GaN:Er samples synthesized by pulsed growth. It can be seen from Fig. 3 that the sample with higher Er concentration (N_{Er}) exhibits higher emission intensity at $1.5\ \mu\text{m}$, as expected. However, as shown in Fig. 2, the impact of increasing in N_{Er} on the FWHM of the XRD rocking curve of the GaN (0002) peak and hence on the crystalline quality is negligible.

The changes in the refractive index due to Er incorporation were measured by spectroscopic ellipsometry (SE) (alpha-SE Ellipsometer by J.A. Woollam Company). To

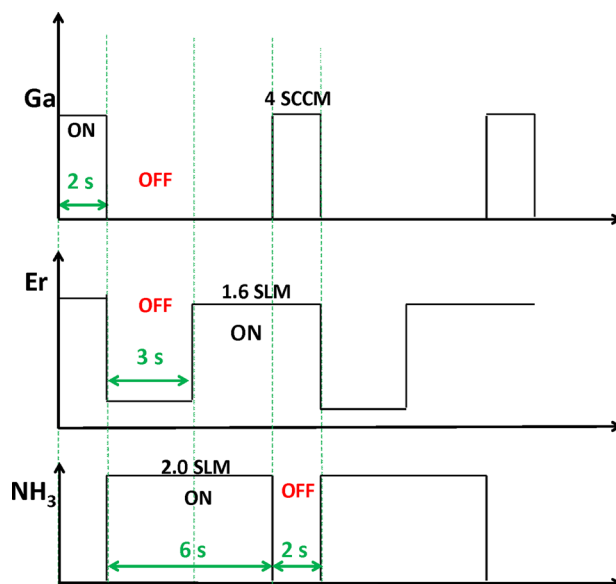


FIG. 1. Schematic of the pulsed precursor flow MOCVD epitaxial growth method for the synthesis of GaN:Er epilayers with alternating supplies of reaction precursors of TRIPeR, TMGa, and NH_3 .

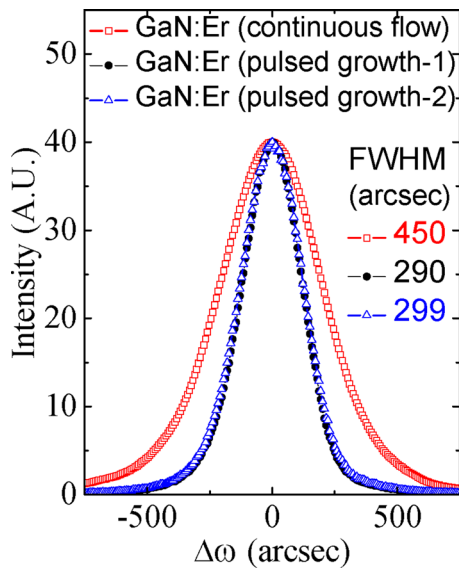


FIG. 2. Comparison of XRD rocking curves (ω -scan) of the GaN (0002) diffraction peak for GaN:Er epilayers grown using pulsed and continuous flow of reaction precursors.

ensure the reliability of the measurement results, the refractive index of the undoped GaN (n_0) was compared to a previous publication²⁷ as well as with the reference data supplied with the SE system. The results shown in Fig. 4 indicate that the measurement results for undoped GaN are consistent with the reference values obtained using the same SE measurement technique.²⁷ Moreover, the raw SE data were fit over a wide spectral range of (385 nm–1600 nm) which adds to the reliability of the determined optical constants.

In Fig. 5(a), we show the measured index of refraction values (n) in the infrared spectral region for an undoped GaN and the two Er doped GaN epilayers. The results indicate that n increases with an increase of the Er doping concentration (N_{Er}) at all wavelengths. Similar behavior has been observed in Er doped Polymethylmethacrylate (PMMA) layers.²⁸ Since 1.54 μm is the wavelength of most interest,

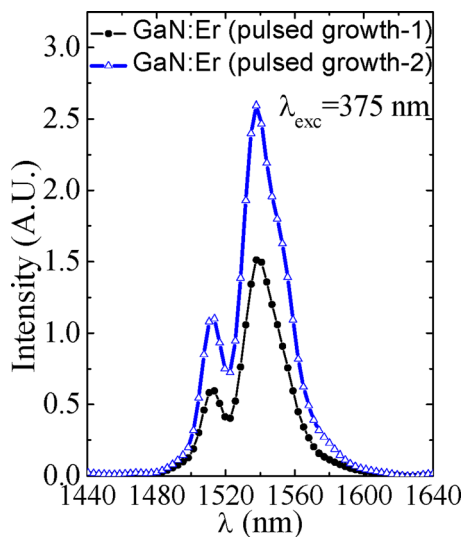


FIG. 3. Room temperature photoluminescence spectra measured around 1.54 μm of two GaN:Er epilayers grown using pulsed method with different Er doping concentrations, $N_{Er} \sim 1.3 \times 10^{20}$ (solid circles) and 3.6×10^{20} (open triangles).

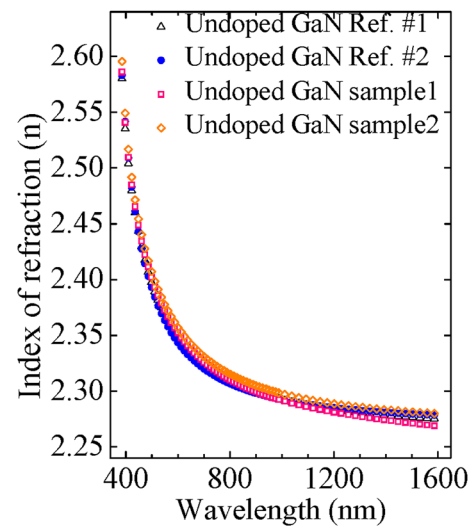


FIG. 4. Comparison of the index of refraction of undoped GaN epilayers of the present work measured by spectroscopic ellipsometry to the reference data. Data for undoped GaN Ref. 1 were supplied with the SE system and data for undoped GaN Ref. 2 were extracted from Ref. 27.

we plot the values of n at 1.54 μm as a function of N_{Er} for these samples, a linear relationship between n_{Er} and N_{Er} is obtained, as shown in Fig. 5(b)

$$n = n_0 + bN_{Er}, \quad (4)$$

where the fitted values of $n_0 = 2.2735$ and $b = 0.00575 \times 10^{-20} \text{ cm}^3$. Knowing this linear dependence will aid in the design of single mode optical waveguide based on GaN:Er epilayers. The increase of index of refraction with N_{Er} stresses the potential use of GaN:Er epilayers as waveguide layers operate at 1.54 while un-doped GaN could be employed as a perfectly lattice matched cladding layer.

In summary, GaN:Er epilayers were prepared by a pulsed precursor flow MOCVD epitaxial technique. The GaN:Er epilayers have significantly improved crystalline quality over similar epilayers grown by the conventional continuous flow of reaction precursors. The index of refraction around the technologically important 1.54 μm wavelength window has been measured and the results showed a linear increase in the index of refraction with increasing Er doping concentration. While the results offer the first order

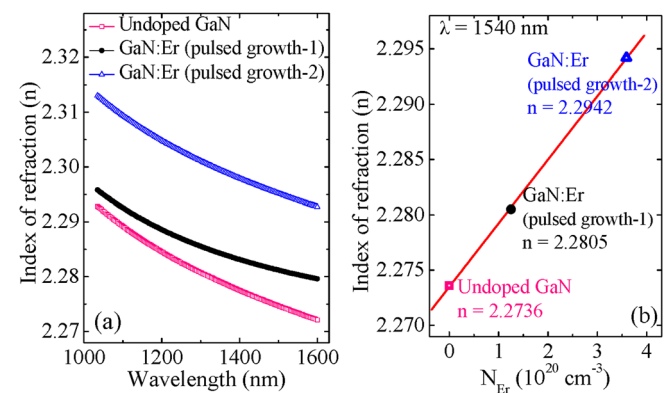


FIG. 5. (a) Index of refraction of undoped and Er doped GaN epilayers obtained from fitting spectroscopic ellipsometry data around the IR region; (b) Index of refraction at 1540 nm plotted as a function of Er concentration (N_{Er}).

information to guide future designs of lasers and optical amplifiers based on Er-doped III-nitride materials, changes in the extinction coefficient or the imaginary part of the refractive index and the optical propagation loss should also be considered in the device design and will be reported in a separate study.

The materials growth effort was supported by JTO/ARO (W911NF-12-1-0330) and the optical characterization work was supported by NSF (ECCS-1200168). Jiang and Lin would like to acknowledge the support of Whitacre Endowed Chairs by the AT & T Foundation. Zavada acknowledges the support from NSF under the IR/D program. Any conclusions in this paper do not necessarily reflect the views of NSF/JTO/ARO.

¹E. Desurvire, *Erbium-Doped Fibre Amplifiers: Principles and Applications* (John Wiley & Sons, 1994).

²R. J. Mears, L. Reekie, I. M. Jauncey, and D. N. Payne, *Electron. Lett.* **23**, 1026 (1987).

³P. C. Becker, N. A. Olsson, and J. R. Simpson, *Erbium-Doped Fibre Amplifiers: Fundamentals and Technology* (Academic Press, 1999).

⁴M. J. Connelly, *Semiconductor Optical Amplifiers* (Springer, 2002).

⁵P. G. Kik and A. Polman, *J. Appl. Phys.* **91**, 534 (2002).

⁶H. Ennen, J. Schneider, G. Pomrenke, and A. Axmann, *Appl. Phys. Lett.* **43**, 943 (1983).

⁷J. Michel, J. L. Benton, R. F. Ferrante, D. C. Jacobson, D. J. Eaglesham, E. A. Fitzgerald, Y. Xie, J. M. Poate, and L. C. Kimerling, *J. Appl. Phys.* **70**, 2672 (1991).

⁸P. N. Favennec, H. L'Haridon, M. Salvi, D. Moutonnet, and Y. Le Guillou, *Electron. Lett.* **25**, 718 (1989).

⁹R. G. Wilson, R. N. Schwartz, C. R. Abernathy, S. J. Pearton, N. Newman, M. Rubin, T. Fu, and J. M. Zavada, *Appl. Phys. Lett.* **65**, 992 (1994).

¹⁰J. T. Torvik, R. J. Feuerstein, J. I. Pankove, C. H. Qiu, and F. Namavar, *Appl. Phys. Lett.* **69**, 2098 (1996).

¹¹S. Kim, S. J. Rhee, D. A. Turnbull, X. Li, J. J. Coleman, S. G. Bishop, and P. B. Klein, *Appl. Phys. Lett.* **71**, 2662 (1997).

¹²M. Garter, J. Scofield, R. Birkhahn, and A. J. Steckl, *Appl. Phys. Lett.* **74**, 182 (1999).

¹³J. M. Zavada, S. X. Jin, N. Nepal, J. Y. Lin, H. X. Jiang, P. Chow, and B. Hertog, *Appl. Phys. Lett.* **84**, 1061 (2004).

¹⁴C. Ugolini, N. Nepal, J. Y. Lin, H. X. Jiang, and J. M. Zavada, *Appl. Phys. Lett.* **89**, 151903 (2006).

¹⁵R. Dahal, C. Ugolini, J. Y. Lin, H. X. Jiang, and J. M. Zavada, *Appl. Phys. Lett.* **93**, 033502 (2008).

¹⁶R. Dahal, C. Ugolini, J. Y. Lin, H. X. Jiang, and J. M. Zavada, *Appl. Phys. Lett.* **95**, 111109 (2009).

¹⁷R. Dahal, C. Ugolini, J. Y. Lin, H. X. Jiang, and J. M. Zavada, *Appl. Phys. Lett.* **97**, 141109 (2010).

¹⁸K. Gerd, *Optical Fiber Communications* (McGraw-Hill, 1998).

¹⁹I. W. Feng, W. P. Zhao, J. Li, J. Y. Lin, H. X. Jiang, and J. Zavada, *Appl. Opt.* **52**, 5426 (2013).

²⁰I. W. Feng, J. Li, J. Y. Lin, H. X. Jiang, and J. M. Zavada, *Opt. Mater. Express* **2**, 1095 (2012).

²¹C. Ugolini, I. W. Feng, A. Sedhain, J. Y. Lin, H. X. Jiang, and J. M. Zavada, *Appl. Phys. Lett.* **101**, 051114 (2012).

²²S. Nakamura, G. Fasol, and S. J. Pearton, *The Blue Laser Diode: The Complete Story* (Springer, New York, 2000).

²³M. A. Khan, J. N. Kuznia, R. A. Skogman, D. T. Olson, M. M. Millan, and W. J. Choyke, *Appl. Phys. Lett.* **61**, 2539 (1992).

²⁴H. J. Kim, S. Choi, D. Yoo, J. H. Ryou, R. D. Dupuis, R. F. Dalmau, P. Lu, and Z. Sitar, *Appl. Phys. Lett.* **93**, 022103 (2008).

²⁵H. X. Jiang and J. Y. Lin, "AlN epitaxial layers for UV photonics," in *Optoelectronic Devices: III-Nitride*, edited by M. Razeghi and M. Heini (Elsevier Ltd., Amsterdam, 2004), Chap 7.

²⁶C. Munasinghe and A. J. Steckl, *Thin Solid Films* **496**, 636 (2006).

²⁷G. Yu, G. Wang, H. Ishikawa, M. Umeno, T. Soga, T. Egawa, J. Watanabe, and T. Jimbo, *Appl. Phys. Lett.* **70**, 3209 (1997).

²⁸V. Prajzler, V. Jerábek, O. Lyutakov, I. Hüttel, J. Špírková, V. Machovič, J. Oswald, D. Chvostová, and J. Zavadil, *Acta Polytech.* **48**, 14 (2008), available at <http://ctn.cvut.cz/ap/index.php?year=2008&idissue=61>.